The role of diffusion-weighted MRI in the classification of liver hydatid cysts and differentiation of simple cysts and abscesses from hydatid cysts

Esra Oruç, Nalan Yıldırım, Naile Bolca Topal, Sadık Kılıçturgay, Semra Akgöz, Gürsel Savcı

PURPOSE
The purpose of this study is to identify the role of diffusion-weighted magnetic resonance imaging (DW-MRI) in the classification of liver hydatid cysts (HCs) and their differentiation from simple cysts and liver abscesses.

MATERIALS AND METHODS
Twenty-two patients that were sent to our department with preliminary diagnoses of HCs or abscess were included in the study. Thirty lesions were evaluated. MRI included T1-weighted fast gradient echo, T2-weighted half-Fourier acquisition single-shot turbo spin echo, and DW single-shot echo planar pulse sequencing (b, 0, 50, and 1000 s/mm²). The apparent diffusion coefficient (ADC) values (mm²/s) of the HCs, abscesses, and simple cysts were calculated.

RESULTS
No statistically significant difference was found between the ADC values of type 1 and 3 ($P > 0.05$) HCs and of simple cysts and type 1 HCs ($P > 0.05$). The ADC values of abscesses were significantly lower than those of type 1 and type 3 HCs, and simple cysts. No statistically significant difference was found between the ADC values of abscesses and type 4 HCs ($P > 0.05$). Type 4 lesions exhibited significantly lower ADC values in comparison to type 1 and 3 HCs.

CONCLUSION
DW-MRI helps differentiate type 4 lesions from other cysts and can distinguish abscesses from hydatid cysts other than type 4 as well as from simple cysts. Type 1 HCs cannot be differentiated from simple cysts using ADC values alone, and type 4 lesions are indistinguishable from abscesses.

Key words: • liver • echinococcosis • magnetic resonance imaging • diffusion weighted MRI

From the Departments of Radiology (E.O., N.Y. ✉ nalanmed76@hotmail.com, N.B.T., G.S.), and General Surgery (S.K.), Uludağ University School of Medicine, Bursa, Turkey; and the Department of Biostatistics (S.A.), Çanakkale Onsekiz Mart University School of Medicine, Çanakkale, Turkey.

Echinococcosis (hydatidosis) is a parasitosis that is endemic in European, Middle Eastern, Mediterranean, South American, and African countries (1). The incidence in Turkish society is reported as 1/2000 (2).This parasitic disease can involve all organs, although it preferentially affects the liver (50–70%) and lungs (20–30%) (3). Ultrasonography (US) is the tool of choice for diagnosis, although computed tomography (CT), magnetic resonance imaging (MRI), and serological tests are also frequently used. According to Gharbi's classification of hydatid cysts (HCs), five subtypes have been defined by sonographical characteristics (Table 1). Although this classification is widely accepted, it has been restandardized by the WHO-Informal Working Group in Echinococcosis (WHO-IWGE) (Table 1). Type 1 HCs comprise 25–40% of all cysts and may be difficult to distinguish from simple cysts due to their sonographic similarity (4). Type 4 HCs can also present diagnostic problems due to their irregular contour, heterogeneous echo pattern, and tumor-like appearance. Type 4 HCs may not be differentiated from intrahepatic collections if a hypoechoic pattern is dominant.

It is well known that routine MRI sequences do not adequately differentiate type 1 HCs from simple cysts. Diffusion-weighted MRI (DW-MRI) is a technique that is sensitive to molecular diffusion in tissues and has commonly been used in brain imaging. This technique has long been limited to the brain imaging due to technical problems and sensitivity to motion artifacts. With the advent of faster sequences, DW-MRI has also been applied to abdominal imaging (5). The value of DW-MRI in the differentiation of abscesses from cystic or necrotic tumors and determination of apparent diffusion coefficient (ADC) values of various abdominal organs and liver masses has been explored (6–8). Inan et al. have recently published their study exploring the role of diffusion weighted MR imaging in the differential diagnosis of hydatid liver disease and simple cysts (9).

In this prospective study, DW-MRIs of liver HCs in different maturation phases were obtained with single shot echo planar sequences with different b values, wherein the ADC values of lesions and liver parenchyma were calculated. We aimed to assess the contribution of DW-MRI to the identification of HC subtypes, in addition to their differentiation from abscesses and simple liver cysts.

Materials and methods

Twenty-seven patients, which were sent to our department for US, CT, or MRI with a preliminary diagnosis of liver HC or abscess between January and May 2006, were evaluated. Thirty-seven lesions were detected in this patient group. In this study, one type 2 HC was not included due to inadequate sample size, and six type 5 lesions were not included due to their calcific content affecting the DW-MRI.

Solid mass lesions and lesions with histopathological diagnoses other than abscesses or HC were also excluded. After the exclusion of one type 2 HC and six type 5 HCs, 30 lesions in 22 patients were included in the statistical analysis. None of the patients had liver dysfunction. The study protocol was approved by the institutional review board, and informed consent was obtained from each patient.

HCs were classified as type 1 (n = 10), type 2 (n = 1), type 3 (n = 5), type 4 (n = 5), and type 5 (n = 6) according to Gharbi's sonographic classification. Four of the patients had more than one lesion. The distribution of these lesions was as follows: One patient had five type 1 HCs and one type 2 HC. Another patient had one type 1 and one type 3 HC. One patient had type 3 and type 5 HCs and an abscess. The remaining patient had three simple cysts. Histopathological and serological evaluation revealed 27 HCs, five abscesses, and five simple cysts. All of the abscesses were diagnosed by histopathological sampling. Anechoic lesions were accepted as simple cysts if the patient was clinically asymptomatic and serological tests were negative. Type 2 and type 3 lesions were diagnosed based on their typical appearance at sonography. Sampling was not performed for type 4 lesions with a typical appearance at sonography and with accompanying positive serological results (n = 3). Tru-cut biopsy was performed for two type 4 lesions with suspicious properties.

Imaging was performed with a 1.5 T MR unit (Magnetom Vision Plus; Siemens, Erlangen, Germany) using a linear array polarized body coil. T1-weighted fast gradient echo (TR/TE/FA, 120 ms/4 ms/80°; matrix, 140x256; FOV, 375 mm; NEX, 1; time, 16 s) and T2-weighted half-Fourier acquisition single-shot turbo spin echo (HASTE) (TR/TE/FA, 4 ms/90 ms/150°; matrix, 160x256; FOV, 375 mm; NEX, 1; time, 20 s) were obtained in the axial plane. A DW single-shot echo planar sequence (TR, 5700 ms; TE,139 ms; FOV, 375 mm; matrix, 128x96; NEX, 1) was obtained for all patients with three different b values (0, 50, and 1000 s/mm²) and during one breath hold period. Whole liver parenchyma was examined with an 8-mm slice thickness and 0.25-mm interslice gap in 17 s. No cardiac or respiratory triggering was applied. Patients with suspicious lesions also underwent contrast-enhanced dynamic scanning as a part of the routine imaging protocol.

The entire lesion, from the center to the periphery, was included in the region of interest (ROI) that was selected for ADC measurements. Areas that were far from vessels in the same lobe/segment as the lesion were selected for ADC measurements of the normal liver parenchyma. The sizes of the ROIs were the same for the lesions and the normal parenchyma.

DW-MRI data sets were transferred to another computer and ADC maps were reconstructed with software (Virtuoso, Siemens). ADC values for HCs, abscesses, and simple cysts were calculated by using the following formula:

$$D (x,y,z) = \frac{[\ln (S1(x,y,z) / S2(x,y,z))]}{(b2-b1)} \quad (8).$$

This formula represents an ADC value (mm²/s) for a voxel that is localized at D (x,y,z); S1(x,y,z) is the signal intensity of a voxel at (x,y,z) of a DW image that is obtained with a specific b1 value (b1, 50); and S2 (x,y,z), is the signal intensity of the same voxel in another DW image that is obtained with a specific b2 value (b2, 1000).

Statistical analysis

Statistical analysis was performed using SPSS 13.0 (SPSS Inc., Chicago, USA). ADC values have been presented as average (± standard deviation) and median (interquartile range) values. Kruskal-Wallis and Mann-Whitney U tests were used to compare the distributions of ADC values among cyst groups. Pair-wise comparisons were performed with a Bonferroni adjustment ($P \leq 0.0125$) in order to ensure that the family-wise alpha would not exceed 0.05. To evaluate the performance of ADC levels in cyst diagnosis, receiver operator curve (ROC) analysis was performed. The sensitivities, specificities, positive/negative predictive values, positive likelihood ratios, and areas under the curve (AUC) of the ADC values were calculated. An AUC that is statistically higher than 0.5 indicates good diagnostic test performance. The cut-off values that can be helpful to differentiate hydatid cysts from simple cysts and abscesses and to classify hydatid cysts were determined using the MedCalc demonstration program. Statistical significance was assigned for P values of less than 0.05.

Results

A total of 22 patients (11 men and 11 women) were included in this study. The patients' ages ranged from 22 to 72 years (mean ± SD, 53.9 ± 11.6 years). Thirty lesions were detected in 22 patients and were included in the analysis. The detected lesion diameters ranged from 1.5 cm to 15 cm (mean, 5.9 cm). All ADC measurements were performed without any constraints due to artifacts or lesion diameter. Table 2 depicts the distribution of ADC values (mm²/s) among the detected lesions.

The ADC value of normal liver parenchyma was 0.82×10^{-3} mm²/s. The mean ADC value of simple cysts was $3.08 (\pm 0.17 \times 10^{-3})$ mm²/s, whereas that of type 1 HCs was $2.84 (\pm 0.38)$ mm²/s. There was no statistically significant difference between the ADC values of simple cysts and those of type 1 HCs ($P > 0.05$) (Figs. 1 and 2).

Table 1. Gharbi and WHO-Informal Working Group in Echinococcosis (WHO-IWGE) classification of hydatid cysts

| Gharbi	WHO-IWGE	Sonographic characteristics
-	CL	Unilocular cyst, anechoic, no wall depicted
Type 1	CE1	CL characteristics + wall + mobile internal echogenicities
Type 3	CE2	Multivesicular, multiseptated cyst, daughter cysts, honeycomb pattern
Type 2	CE3	Detached membrane (water-lily sign)
Type 4	CE4	Heterogeneous, hypo-, or hyper-echoic cyst, no daughter vesicles
Type 5	CE5	Cyst with a partial or complete wall calcification

CL, cystic lesion; CE, cystic echinococcosis.
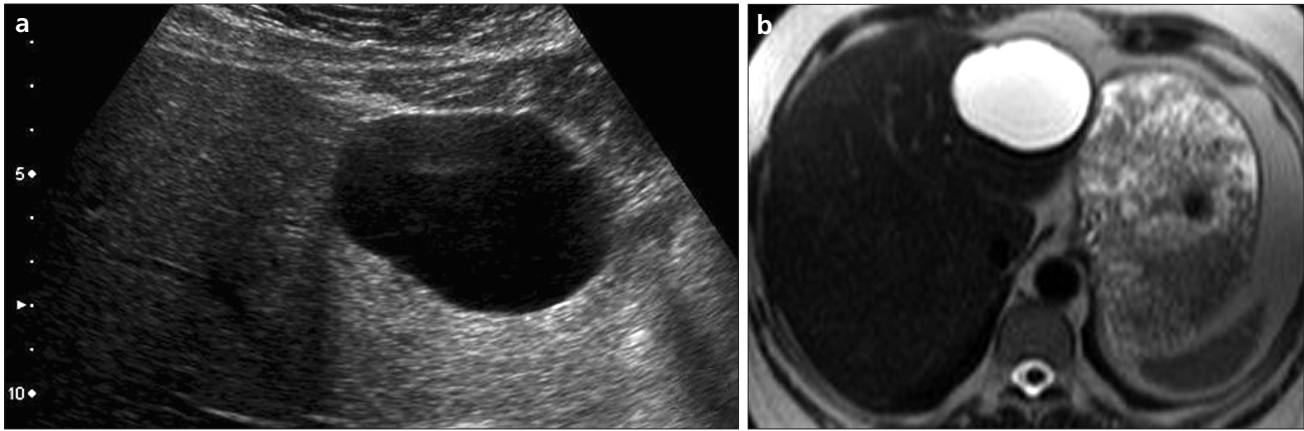
Figure 1. a–d. A simple cyst. US image (a) shows an anechoic mass with posterior acoustic enhancement. Axial T2-weighted HASTE MR image (b) shows the cystic mass in the left lobe of the liver. The lesion is hyperintense with no septae or solid portions. On the diffusion-weighted MR image (c) the lesion exhibits high signal intensity (b = 1000). On apparent diffusion coefficient (ADC) map, ADC value (d) is 3.34×10^{-3}.
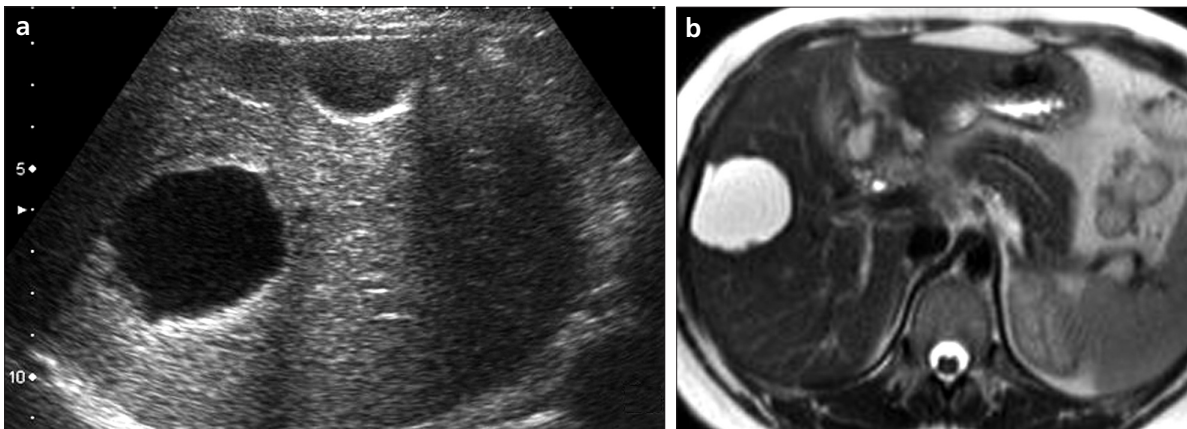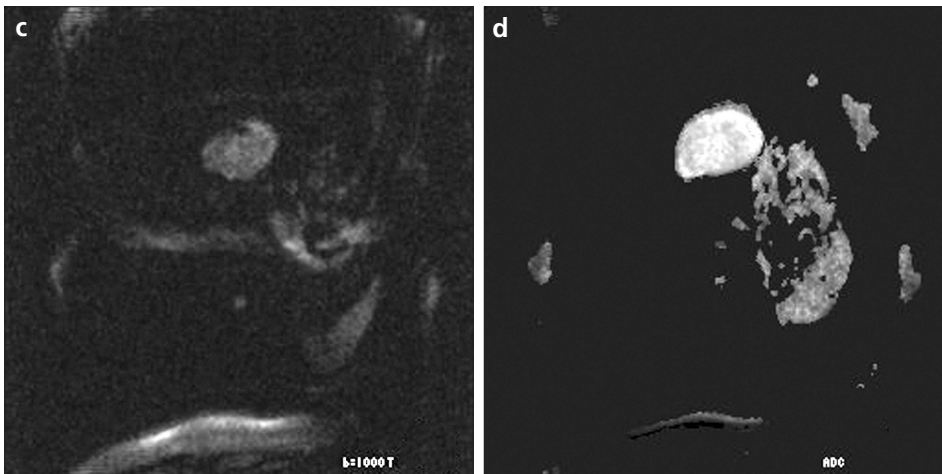

Figure 2. a–d. A type 1 hydatid cyst. US image (a) reveals a round, anechoic lesion with acoustic enhancement. Axial T2-weighted HASTE MR image (b) depicts the same cystic mass in the anterior segment of right lobe of the liver (subsegment 5). The lesion is hyperintense with no septae or solid portions. On the diffusion-weighted MR image (c) the lesion exhibits high signal intensity (b = 1000). On apparent diffusion coefficient (ADC) map (d), ADC value is 2.31×10^{-3}.
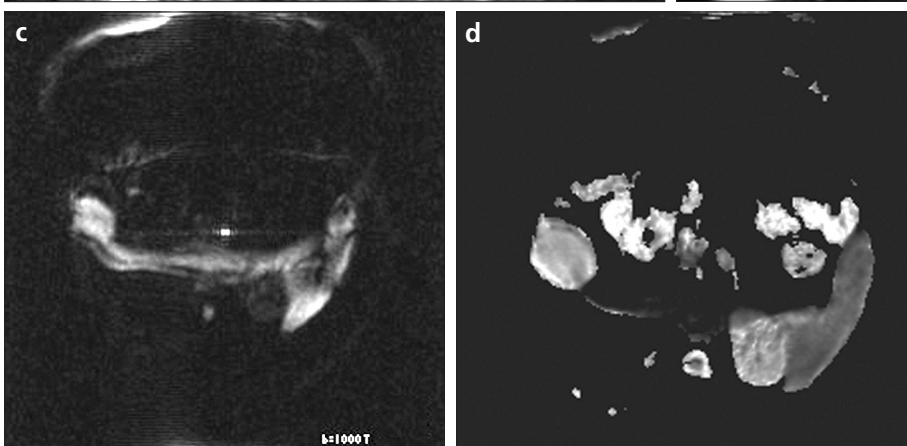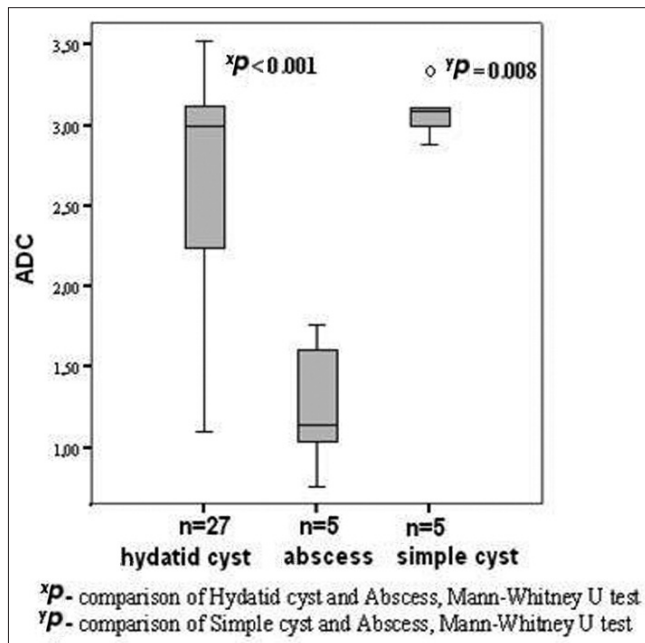
Figure 3. There is a statistically significant difference between the ADC values of abscesses and those of hydatid and simple cysts (*P* = 0.003). The ADC values of abscesses were smaller than those of hydatid cysts and simple cysts (*P* < 0.001 and *P* = 0.008, respectively).

There was a statistically significant difference between the ADC values of abscesses, HCs, and simple cysts (*P* = 0.003). The ADC values of abscesses were significantly lower than those of HCs and simple cysts (*P* = 0.001 and *P* = 0.008, respectively, Fig. 3); however, no statistically significant difference was observed between abscess and type 4 HC ADC values (*P* > 0.05) (Table 2, Figs. 4 and 5).

There was a statistically significant difference between the ADC values of different types of HCs (*P* = 0.006). Because there was only one type 2 HC, it was not included in the analysis. Type 4 HCs exhibited significantly lower ADC values in comparison to type 1 and 3 HCs (Table 2). No statistically significant difference was found between type 1 and 3 HC ADC values (*P* > 0.05).

The diagnostic performance level of DW-MRI for liver HC subtyping was evaluated via ROC analysis. DW-MRI was found to be successful in the differentiation of type 4 HCs from other types (AUC, 0.987; 95% CI, 0.816–1.000). The highest accuracy for type 4 HCs was obtained with ADC value of ≤ 2.17×10^{-3} mm^2/s (Table 3). When a cut-off value of ≤ 2.17 was used, one type 1 HC and all of the abscesses were diagnosed as type 4 HCs (Fig. 6).

DW-MRI was also successful in the differentiation of HCs from abscesses (AUC, 0.952; 95% CI, 0.789–0.994). The highest accuracy for HC differen-

tiation was obtained with ADC values of >1.76×10^{-3} mm^2/s (Table 3). For this ADC cut off value, two out of five type 4 HCs were diagnosed as abscesses (Figs. 7 and 8).

DW-MRI was not successful in the differentiation of HCs from simple cysts (AUC, 0.705; 95% CI, 0.495–0.865) (Table 3).

Discussion

Parasitic diseases are an important health problem in developing countries. Hydatidosis (echinococcosis) is one of the most important parasitic diseases that threaten human and animal health in both Turkey and throughout the world. The large number of cattle herds in Turkey, in addition to the human-dog cycle, is responsible for the increased prevalence of this infestation.

US is the gold standard imaging method for HC categorization. US provides information of both the number and location of cysts, the relationships of cysts to adjacent structures, and the inner structures of the cysts/lesions. Typical findings, such as the anechoic inner contents, germinative membranes, honeycomb or spoke-wheel patterns, or wall calcifications of type 1, 2, 3, and type 5 lesions, respectively, are easily recognized. On the other hand, the differentiation of type 1 lesions from simple cysts and type 4 lesions from other solid lesions of the liver can cause diagnostic dilemmas. CT and MRI can be performed when diagnosis is not possible with US alone. A pericyst, due to its fibrous component and calcification, is depicted as a hypointense rim on T1- and T2-weighted images (10). MRI can be helpful in identifying the rim and differentiating this diagnosis from other encapsulated

Table 2. Distribution of apparent diffusion coefficient (ADC) values with respect to lesions

		Type 1 (n = 10)	Type 3 (n = 5)	Type 4 (n = 5)	Abscess (n = 5)	Simple cyst (n = 5)
ADC value	mean ± SD (min.–max.)	2.84 (±0.38) (2.15–3.18)	3.05 (±0.17) (2.91–3.35)	1.78 (±0.44) (1.10–2.17)	1.26 (±0.41) (0.76–1.76)	3.08 (±0.17) (2.89–3.34)
P[a] value	Comparison to type 4	*P* = 0.001	*P* = 0.008		*P* = 0.151	*P* = 0.008
	Comparison to abscess	*P* = 0.001	*P* = 0.008	*P* = 0.151		*P* = 0.008

[a]Mann-Whitney U test (a *P* value ≤ 0.0125 was accepted as statistically significant with Bonferroni adjustment); SD, standard deviation.
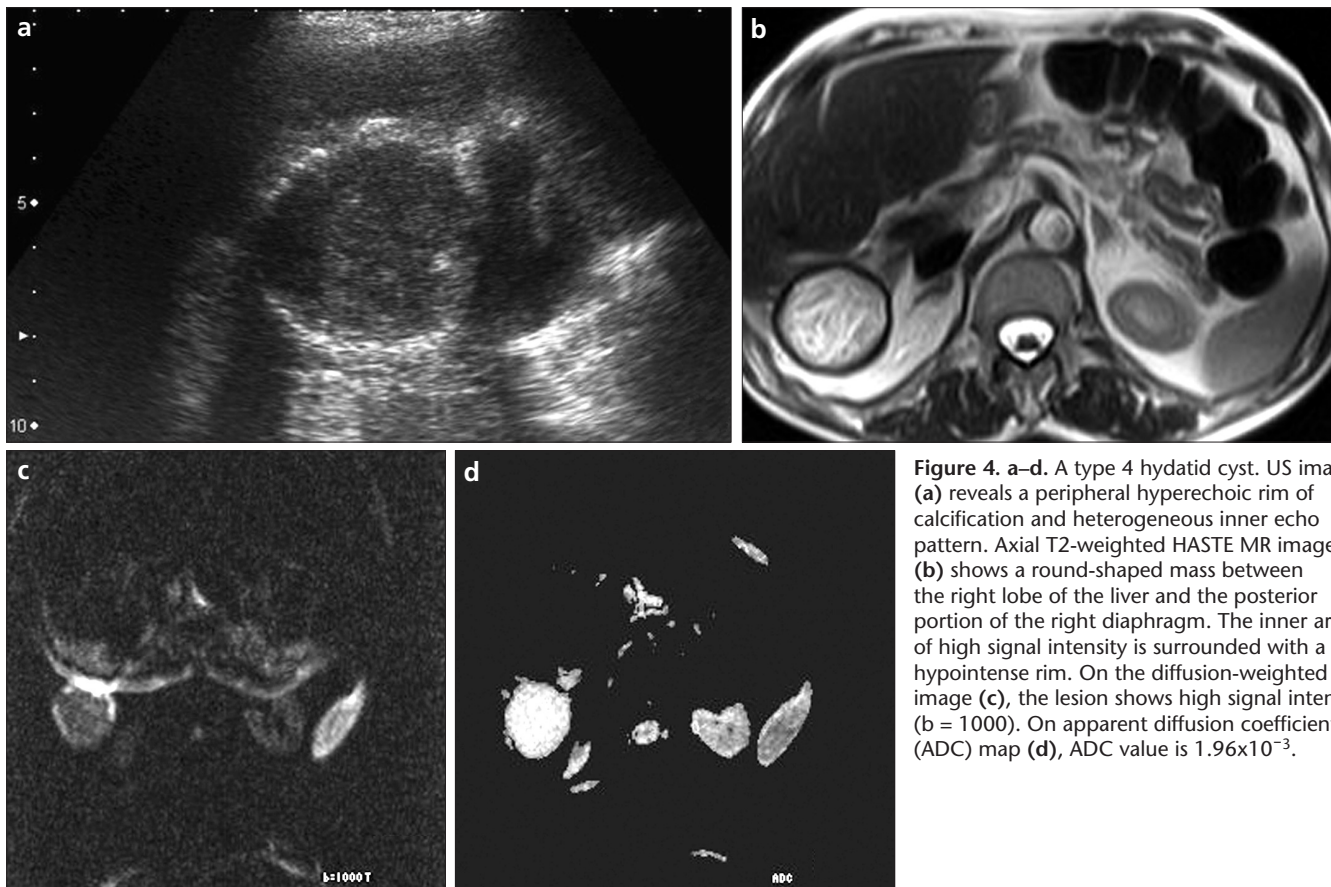
Figure 4. a–d. A type 4 hydatid cyst. US image (**a**) reveals a peripheral hyperechoic rim of calcification and heterogeneous inner echo pattern. Axial T2-weighted HASTE MR image (**b**) shows a round-shaped mass between the right lobe of the liver and the posterior portion of the right diaphragm. The inner area of high signal intensity is surrounded with a hypointense rim. On the diffusion-weighted MR image (**c**), the lesion shows high signal intensity (b = 1000). On apparent diffusion coefficient (ADC) map (**d**), ADC value is 1.96×10^{-3}.
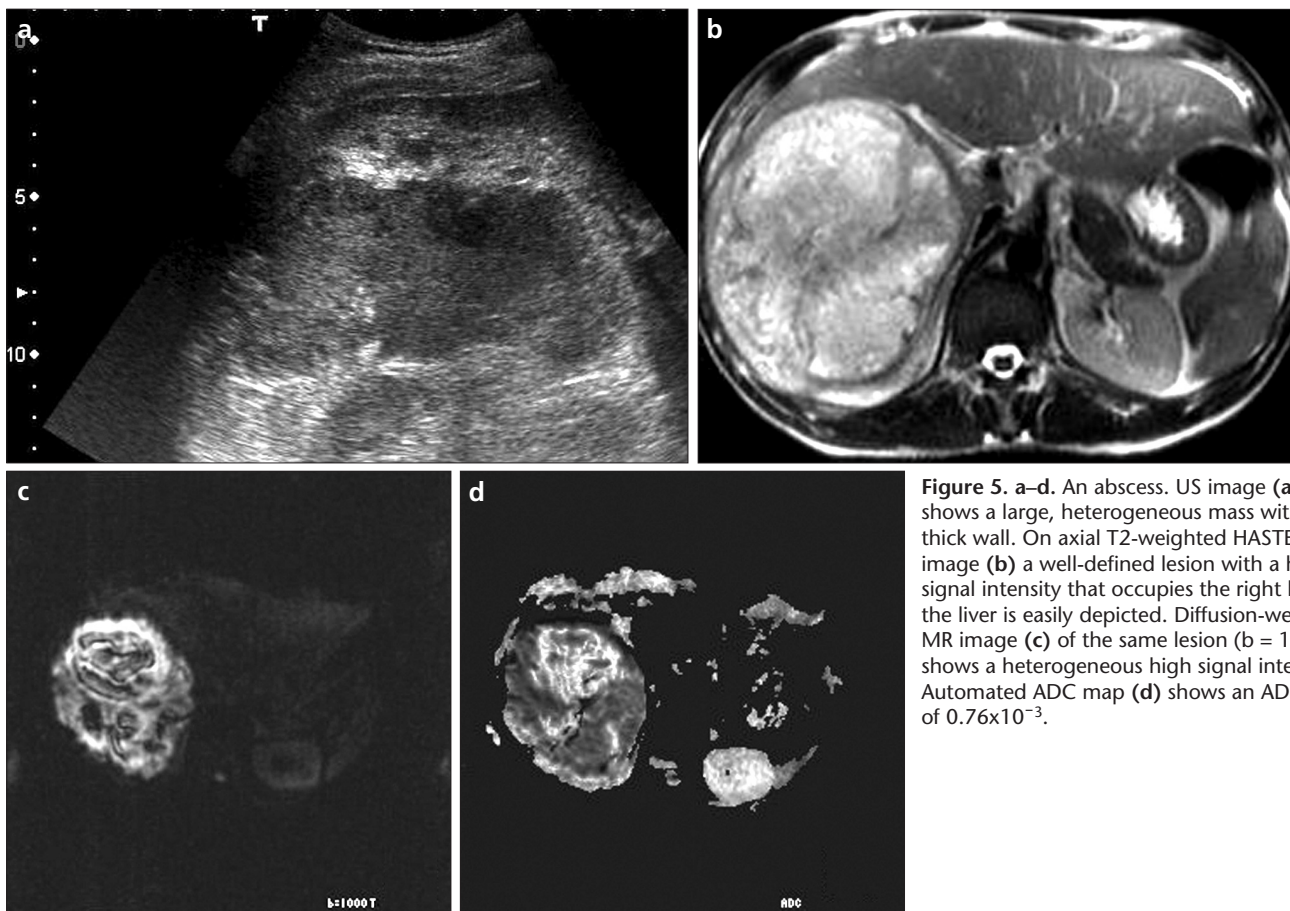

Figure 5. a–d. An abscess. US image (**a**) shows a large, heterogeneous mass with a thick wall. On axial T2-weighted HASTE MR image (**b**) a well-defined lesion with a high signal intensity that occupies the right lobe of the liver is easily depicted. Diffusion-weighted MR image (**c**) of the same lesion (b = 1000) shows a heterogeneous high signal intensity. Automated ADC map (**d**) shows an ADC value of 0.76×10^{-3}.
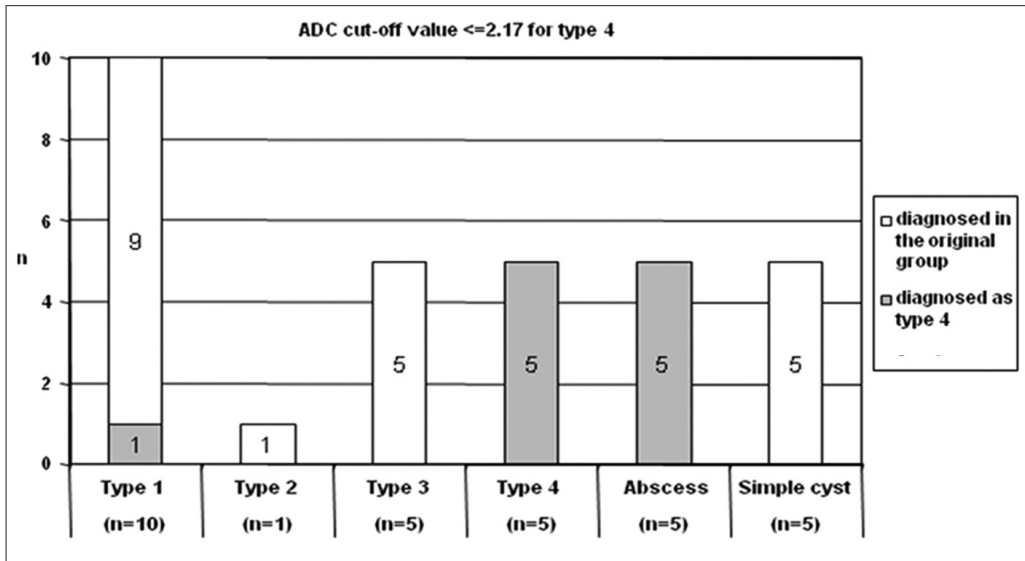
Figure 6. When the cut-off value is accepted as ≤2.17 for type 4 hydatid cysts, all of the abscesses and one type 1 hydatid cyst were also diagnosed as type 4 hydatid cysts. The others were diagnosed correctly (in the original group) by using this cut-off value.
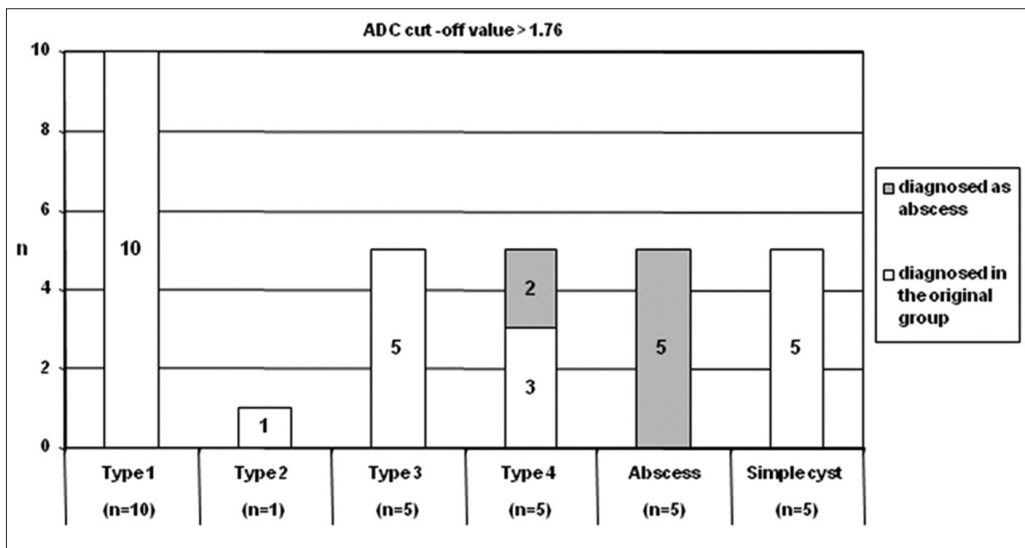

Figure 7. When the cut-off value is accepted as >1.76, two of the type 4 hydatid cysts were also diagnosed as abscesses. The others were diagnosed correctly (in the original group) by using this cut-off value.

Table 3. Diagnostic performance of apparent diffusion coefficient s (ADCs) for differentiating type 4 from other types of hydatid cysts, hydatid cysts from abscesses, and hydatid cysts from hydatid cysts

	Type 4 (n = 5) versus other hydatid cysts (n = 16)	Hydatid cysts (n = 21) versus abscess (n = 5)	Hydatid cysts (n = 21) versus simple cysts (n = 5)
Cut-off value	≤2.17	>1.76	≤2.74
Sensitivity (%)(95% CI)	100 (48–100)	90.5 (69.6–98.5)	47.6 (25.7–70.2)
Specificity (%)(95% CI)	93.7 (69.7–99)	100 (48–100)	100 (48–100)
Positive predictive value (%)	83.3	100	100
Negative predictive value (%)	100	71.4	31.3
Positive likelihood ratio	16	- a	- a
Area under curve (95% CI)	0.987 (0.816–1.000)	0.952 (0.789–0.994)	0.705 (0.495–0.865)

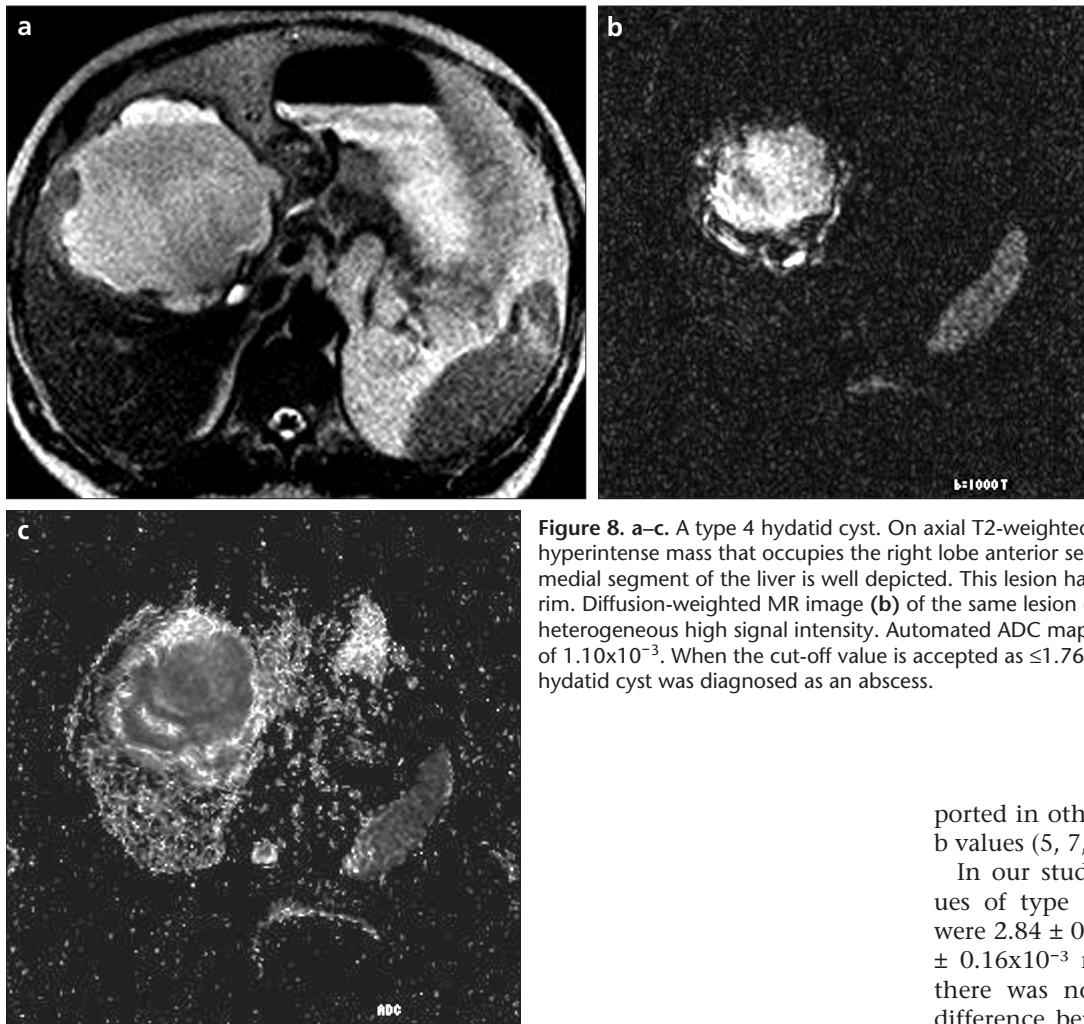a not calculated due to 100% specificity; CI, confidence interval.

Figure 8. a–c. A type 4 hydatid cyst. On axial T2-weighted HASTE MR image **(a)** the hyperintense mass that occupies the right lobe anterior segment and the left lobe medial segment of the liver is well depicted. This lesion has an irregular hypointense rim. Diffusion-weighted MR image **(b)** of the same lesion (b = 1000) exhibits a heterogeneous high signal intensity. Automated ADC map **(c)** shows an ADC value of 1.10×10^{-3}. When the cut-off value is accepted as ≤1.76 for abscesses, this type 4 hydatid cyst was diagnosed as an abscess.

liver lesions. Irregularities of the rim border, which can be accepted as signs of partial detachment, are more reliably demonstrated with MRI than with CT or US (11).

Differential diagnoses can be more accurately made with MRI when characteristic features of HCs, like hydatid sand, daughter vesicles, or calcified membrane, do not exist (12).

Owing to the reasons mentioned above, an easy and practical diagnostic method is needed for daily practice.

In our study, we evaluated the diagnostic value of DW-MRI in the subtyping of HCs and their differentiation from abscesses and simple cysts. Moteki et al. was the first to use this technique in the abdomen in 1994, wherein they assessed abdominal organs and muscle tissue (13). In following years, several studies concerning the contribution of DW-MRI in the evaluation of abdominal organs and the ADC values of abdominal organs have been published

(5–8, 14–18); however, the number of papers exploring the value of DW-MRI in the diagnosis of hydatid liver disease is limited (9).

Diffusion is either isotropic or anisotropic in environments with randomly organized microstructures or without any organized barriers to the motion of molecules and with microstructures organized in one predominant direction, respectively. Taouli et al. have demonstrated that diffusion in the liver is isotropic (15). The ADC is used in order to describe the impact of signal loss due to water diffusion, intravascular blood flow, CSF flow, and cardiac pulsations, as well as tissue temperature and magnetic susceptibility, on the diffusion coefficient. As fast imaging sequences have emerged, it has become possible to use DW-MRI in the abdomen as well. In our study, the average ADC value of normal liver parenchyma was 0.82×10^{-3} mm^2/s, which agrees well with the ADC values that have been re-

ported in other studies that used high b values (5, 7, 14).

In our study, the average ADC values of type 1 HCs and simple cysts were $2.84 \pm 0.38 \times 10^{-3}$ mm^2/s and $3.08 \pm 0.16 \times 10^{-3}$ mm^2/s, respectively, and there was no statistically significant difference between these values so as to differentiate of these lesions (AUC, 0.705; 95% CI, 0.495–0.865). Simple cysts have watery contents without structures that limit the diffusion of water molecules. Type 1 HCs are characterized by walls and multiple echogenic foci, which are caused by hydatid sand, and the latter may be seen within the lesion by repositioning the patient during sonography (19, 20). Dissimilarities in macromolecular or lipid contents and the chemical compositions of lesions are also not distinguishable by DW-MRI. On the contrary, Inan et al. have observed that all HCs, with the exception of two, are significantly hyperintense on DW-MRI (b = 20, b = 1000), whereas simple cysts are not (9). The same group also found that the ADC values of HCs (CE types 1, 2, and 3, and liquid type) were significantly lower than those of simple cysts; however, they were not able to define a cut-off value with ROC analysis. The differences between these two studies might be due to different equipment and sample sizes.

Similarly, type 1 and 3 HCs cannot be distinguished using ADC values. Type 3 HCs are multivesicular, multiseptated cysts, wherein the daughter cysts may partially or completely fill the unilocular mother cyst. Cyst septations may produce wheel-like structures (19). When daughter cysts are separated by a hydatid matrix (a material with mixed echogenicity), they demonstrate a "wheel spoke" pattern. This matrix consists of a hydatid fluid that contains the membranes of broken daughter vesicles, scolices, and hydatid sand (21). Type 3 HCs with these properties show ADC values that are similar to those of type 1 HCs. On the other hand, it may be argued that type 1 lesions that lack water diffusion-limiting structures can also have ADC values that differ from those of type 3 HCs. Type 4 HCs have heterogeneous hypoechoic or dishomogeneous degenerative contents (especially membranes) without daughter cysts (19). Membranes may appear within the matrix as serpentine linear structures, which is a finding that is highly specific for hydatid disease. When the matrix completely fills the cyst, a mixed echogenic pattern that mimics a solid mass is created (21).

DW-MRI successfully differentiates HCs from abscesses (AUC = 0.952; 95% CI = 0.789–0.994). The highest accuracy for HC differentiation was obtained with an ADC value of $>1.76 \times 10^{-3}$ mm^2/s. For an ADC cut-off value of >1.76 mm^2/s, two out of five type 4 HCs were diagnosed as abscesses. We have also shown that the ADC values of abscesses are significantly lower than those of HCs and simple cysts ($P = 0.001$ and $P = 0.008$, respectively). Abscesses contain inflammatory cells, bacteria, necrotic tissues, and highly cellular and viscous proteinaceous exudate, which restrict diffusion and result in low ADC values (16). The mean ADC value for abscesses has been reported to be $1.09 \pm 0.32 \times 10^{-3}$ mm^2/s in the literature (17). The mean ADC value for abscesses in our study was $1.06 \pm 0.41 \times 10^{-3}$ mm^2/s, which is consistent with the aforementioned value from literature. No statistically significant difference was found between the ADC values of type 4 HCs and abscesses ($P > 0.05$). Chan et al. have reported the ADC value for abscesses to be $0.67 \pm 0.35 \times 10^{-3}$ mm^2/s and they have successfully distinguished them from cystic necrotic tumors. They attribute this diversity to a variety of biochemical components and viscosities (16). Bruegel et al. have described the time-dependent change in ADC values of multiple liver lesions in a 36-year-old patient (18). In this study, at admission, ADC values were observed to range from 1.2 to 1.6×10^{-3} mm^2/s, whereas twelve days later, a significant decrease in ADC values to $0.3–0.7 \times 10^{-3}$ mm^2/s was observed. Thus, it is possible to obtain different ADC values during abscess evolution.

The diagnostic performance of DW-MRI imaging for liver HC subtyping was evaluated with ROC analysis. DW-MRI successfully differentiated type 4 HCs from other HC types (AUC, 0.987; 95% CI, 0.816–1.000). The highest accuracy for type 4 HC differentiation was obtained with ADC values ≤ 2.17×10^{-3}. No statistically significant difference was found when the ADC values of HCs and simple cysts were compared (AUC, 0.705; 95% CI, 0.495–0.865).

The ADC values of in vivo structures are usually higher than expected, which is an effect that is generally attributed to capillary microcirculation. Yamada et al., in their article about the contribution of perfusion to the ADC value, have reported that low b values are sensitive to perfusion, which result in falsely elevated parenchymal organ and muscle tissue ADC values (14). They calculated the "true diffusion coefficient" value with a method excluding the contribution of perfusion. They also showed that ADC values of liver, spleen, kidney, pancreas and muscle were higher than the "true diffusion coefficient" which clearly supports the effect of perfusion causing overestimation of ADC values. The "true diffusion coefficient" and ADC values (0 or near 0) were similar for water phantoms, ascites, and gallbladder tissue lacking significant perfusion. Because small b values include the effects of both diffusion and perfusion, the resultant calculated ADC values are higher. Since small b values are more sensitive to perfusion and the T2 values of tissues, high b values are recommended for abdominal diffusion imaging. The applications of different b values in different studies have resulted in varying ADC values (8, 14). Ichikawa et al. have used small b values and obtained a high image quality that cannot be achieved with higher b values (8). In our study, the ADC values can be assumed to depend on water diffusion in the lesions because no perfusion is present and high b values have been used. For this same reason, we made no technical change to diminish the effect of perfusion. On the contrary, abscesses and primary/secondary liver masses that can be difficult to distinguish from type 4 HCs can exhibit circumferential or intra-tumoral perfusion, respectively. Thus, sets of images that are obtained using different b values, which are sensitive to perfusion, diffusion, or both, can aid in differential diagnosis.

There are some limitations of our study. The most significant limitation of this study is the small patient number. Studies with more patients would result in a higher significance level, although our results suggest trends. Because only one patient presented with a type 2 HC, we were unable to include type 2 patients in our analysis. A large series including other cystic liver lesions would provide more information. Separate calculation of the diffusion coefficient and perfusion fraction can aid in the differentiation of type 4 HCs and vascular lesions. It is also difficult to compare our results to previously published results because the technical equipment and parameters used therein considerably vary.

In conclusion, DW-MRI is helpful for the differentiation of type 4 HCs from other cysts and abscesses, from type 1, 2, and 3 HCs, and from simple cysts. Type 1 HCs cannot be differentiated from simple cysts with ADC values.

References

1. Ammann RW, Eckert J. Cestodes echinococcus. Gastroenterol Clin North Am 1996; 25:655–689.
2. Aytac A, Yurdakul Y, İkizler C, et al. Pulmonary hydatid disease: report of 100 patients. Ann Thorac Surg 1997; 23:145–513.
3. Khuroo MS, Wani NA, Javid G, et al. Percutaneous drainage compared with surgery for hepatic hydatid cysts. N Eng J Med 1997; 337:881–887.
4. Caremani M, Lapini L, Caremani D, Occhini U. Sonographic diagnosis of hydatidosis: the sign of the cyst wall. Eur J Ultrasound 2003; 16:217–223.
5. Kim T, Murakami T, Takahashi S, Hori M, Tsuda K, Nakamura H. Diffusion-weighted single-shot echo planar MR imaging for liver disease. AJR Am J Roentgenol 1999; 173:393–398.
6. Muller MF, Prasad P, Siewert B, Nissenbaum MA, Raptopoulos V, Edelman R. Abdominal diffusion mapping with use of a whole-body echo-planar system. Radiology 1994; 190:475–483.

7. Namimoto H, Yamashita Y, Sumi S, Tang Y, Takahashi M. Focal liver masses: characterization with diffusion-weighted echo-planar MR imaging. Radiology 1997; 204:739–744.

8. Ichikawa T, Haradome H, Hachiya J, Nitatori T, Araki T. Diffusion-weighted MR imaging with single-shot echo planar imaging in the upper abdomen: preliminary clinical experience in 61 patients. Abdom Imaging 1999; 24:456–461.

9. Inan N, Arslan A, Akansel G, et al. Diffusion-weighted imaging in the differential diagnosis of simple and hydatid cysts of the liver. AJR Am J Roentgenol 2007; 189:1031–1036.

10. Adapinar B. Manyetik rezonans görüntüleme fiziği. In: Temel Radyoloji Tekniği. Kaya T, ed. Bursa: Güneş&Nobel, 1997; 355–393.

11. Marani D. A, Canossi GC, Nicoli FA, Alberti GP, Monni SG, Casolo PM. Hydatid disease: MR imaging study. Radiology 1990; 175:701–706.

12. Oyar O, Gülsoy UK. Tıbbi görüntüleme fiziği. Ankara: Tisamat, 2003; 291–360.

13. Moteki T, Horikoshi H, Oya N, Aoki J, Endo K. Evaluation of hepatic 298 lesions and hepatic parenchyma using diffusion weighted reordered turbo FLASH magnetic resonance images. JMRI 2002; 15:564–572.

14. Yamada I, Aung W, Himeno Y, Nakagawa T, Shibuya H. Diffusion coefficients in abdominal organs and hepatic lesions: evaluation with intravoxel incoherent motion echo303 planar MR imaging. Radiology 1999; 210:617–623.

15. Taouli B, Vilgrain V, Dumont E, Daire JL, Fan B, Menu Y. Evaluation of liver diffusion isotropy and characterization of focal hepatic lesions with two single-shot echo-planar MR imaging sequences: prospective study in 66 patients. Radiology 2003; 226:71–78.

16. Chan JHM, Tsui EYK, Luk HS, et al. Diffusion weighted MR imaging of the liver: distinguishing hepatic abscess from cystic or necrotic tumor. Abdom Imaging 2001; 26:161–165.

17. Demir OI, Obuz F, Sağol O, Dicle O. Contribution of diffusion-weighted MRI to the differential diagnosis of hepatic masses. Diagn Interv Radiol 2007; 13:81–86.

18. Bruegel M, Holzapfel K, Gaa J, et al. Characterization of focal liver lesions by ADC measurements using a respiratory triggered diffusion-weighted single-shot echo-planar MR imaging technique. Eur Radiol 2008; 18:477–485.

19. WHO Informal Working Group. International classification of ultrasound images in cystic echinococcosis for application in clinical and field epidemiological settings. Acta Trop 2003; 85:253–261.

20. Yuksel M, Demirpolat G, Sever A, Bakaris S, Bulbuloglu E, Elmas N. Hydatid disease involving some rare locations in the body: a pictorial essay. Korean J Radiol 2007; 8:531–540.

21. Pedrosa I, Saiz A, Arrazola J, Ferreiros J, Pedrosa CS. Hydatid disease: radiologic and pathologic features and complications. RadioGraphics 2000; 20:795–817.